

**\*\*TITLE\*\***

ASP Conference Series, Vol. **\*\*VOLUME\*\***, **\*\*PUBLICATION YEAR\*\***

**\*\*EDITORS\*\***

## **Simultaneous Measurements of the Fried Parameter $r_0$ and the Isoplanatic Angle $\theta_0$ using SCIDAR and Adaptive Optics - First Results**

A.R. Weiß, S. Hippler, M.E. Kasper

*Max-Planck-Institut für Astronomie, Königstuhl 17, 69117 Heidelberg, Germany*

N.J. Wooder, J.C. Quartel

*Blackett Lab, Imperial College, SW72BZ London, United Kingdom*

**Abstract.** We present first results of a simultaneous atmospheric turbulence measurement campaign at the Calar Alto (Spain) 1.23 m and 3.5 m telescopes. A SCIDAR instrument and the Calar Alto Adaptive Optics system ALFA were used at the 1.23 m and 3.5 m telescopes respectively to determine essential turbulence parameters like the Fried parameter  $r_0$ , the isoplanatic angle  $\theta_0$ , and, in the case of SCIDAR, the  $C_n^2$  profile of the atmosphere. Both closed-loop and open-loop data were obtained with ALFA. The desired parameters were then calculated from this. This paper shows a comparison of the results obtained from the two different systems for several times during a period of three nights.

### **1. Introduction**

The quality of correction and the overall quality of the images achievable by the use of Adaptive Optics (AO) is strongly dependent on the momentary properties of atmospheric turbulence as well as a good adjustment of instrumental parameters (such as spatial and temporal sampling rates) to these properties. A measure for the quality of the AO correction is the shape of the point spread function (PSF) of a given instrument at a given time. Experience shows that the PSF is subject to rapid variations that originate in the stochastic nature of atmospheric turbulence as well as in instrumental limitations. Veran et al. (1997) have shown, that it is possible to retrieve the shape of an on-axis long-exposure PSF from the measurements of a curvature AO system. This PSF can then be used for the reconstruction and reduction of AO compensated image data. Our goal is to apply a similar method to the Calar Alto AO system ALFA and — if possible — reconstruct the PSF not only on-axis but also to give an approximation of off-axis PSFs over the whole field of view. Additionally we want to optimize the closed-loop parameter selection process by using additional information on the momentary state of atmospheric turbulence. For this purpose we conducted a measurement campaign at the Calar Alto 1.23 m and 3.5 m telescopes using a SCIDAR instrument and ALFA, respectively, in order to determine the amount of information that is encoded in wave front measurements as well as to establish the benefit of simultaneous SCIDAR measurements when using an AO system. The two instruments will be described more closely in the next section.

## 2. The Instruments

### 2.1. SCIDAR

SCIDAR (Scintillation Detection And Ranging) is a technique to determine vertical profiles of atmospheric turbulence properties such as  $C_n^2(h)$ ,  $\tau_o(h)$  and  $\vec{v}(h)$  from pupil plane measurements of double star's scintillations (Rocca, Roddier, & Vernin, 1974). While the first SCIDAR instruments measured scintillation at ground level and were therefore not sensitive below a given height (depending on Fresnel propagation heights) an improvement first proposed by Fuchs, Tallon, & Vernin (1994) that basically results in measuring scintillation patterns virtually several kilometers *below* ground level makes ground level turbulence accessible to SCIDAR measurements. This technique is mostly referred to as *generalized* SCIDAR. The generalized SCIDAR instrument used in our measurements was developed and built by Imperial College's Applied Optics Group at Blackett Lab in London. It has a relatively simple setup and can therefore be easily transported. The instrument consists of a light intensifier that is fibre-coupled to a CCD camera. The main lens is chosen such that pixel sampling in the pupil plane of the telescope is approximately  $1 \times 1 \text{ cm}^2$ . For the generalized SCIDAR mode, lenses can be selected for different positions of the conjugate plane. Data are recorded with a pixel exposure time of 1.0 ms and a frame rate of 305 Hz. Due to the high data rate and limited disk space, the measurements are written to tape and reduced later (one 32 MByte block of data of each run is processed in near real-time in order to get an approximate  $C_n^2(h)$  profile). Figure 1 shows a front view of the instrument mounted on the Calar Alto 1.23 m telescope.

### 2.2. ALFA and OMEGA-Cass

ALFA is a Shack-Hartmann (SH) type AO system (Hippler et al. 1998; Kasper et al. 2000). Its AO subsystem consists of the SH Wavefront Sensor (SHWFS), a 97 actuator deformable mirror and a real-time control system based on digital signal processors. The SHWFS is capable to correct wavefronts with a frequency between 25 and 1200 Hz, while wavefront sampling can be adjusted using a variety of lenslet arrays (Kasper 2000). Closed-loop correction is realized by modal control of the 97-element deformable mirror (Wirth et al. 1998) with its conjugate plane in the telescope's pupil. Natural guide stars (NGS) or an artificial sodium layer laser guide star (LGS) can be used as a reference for wavefront correction. In the past we regularly achieved Strehl ratios in the range of 20–30% for NGSs while with LGSs a Strehl of 20% was achieved only once so far. While ALFA in NGS mode can now be used as a common user instrument, LGS operation remains problematic. Hence, LGSs were not used in the measurements presented here and will in the future only be available for test purposes. Corrected and uncorrected images of the binaries were obtained by MPIA's OMEGA-Cass near-infrared camera. The camera supports image plane samplings at 0.04–0.12'' per pixel with a  $1024 \times 1024$  near-infrared HAWAII detector. All images here were recorded with a sampling of 0.08'' per pixel in the infrared K-Band, hence the diffraction limited PSF is sufficiently sampled. Figure 2 shows ALFA and OMEGA-Cass mounted on the Calar Alto 3.5 m telescope.



Figure 1. The generalized SCIDAR instrument (bottom center) mounted at the Cassegrain flange of the 1.23 m telescope.

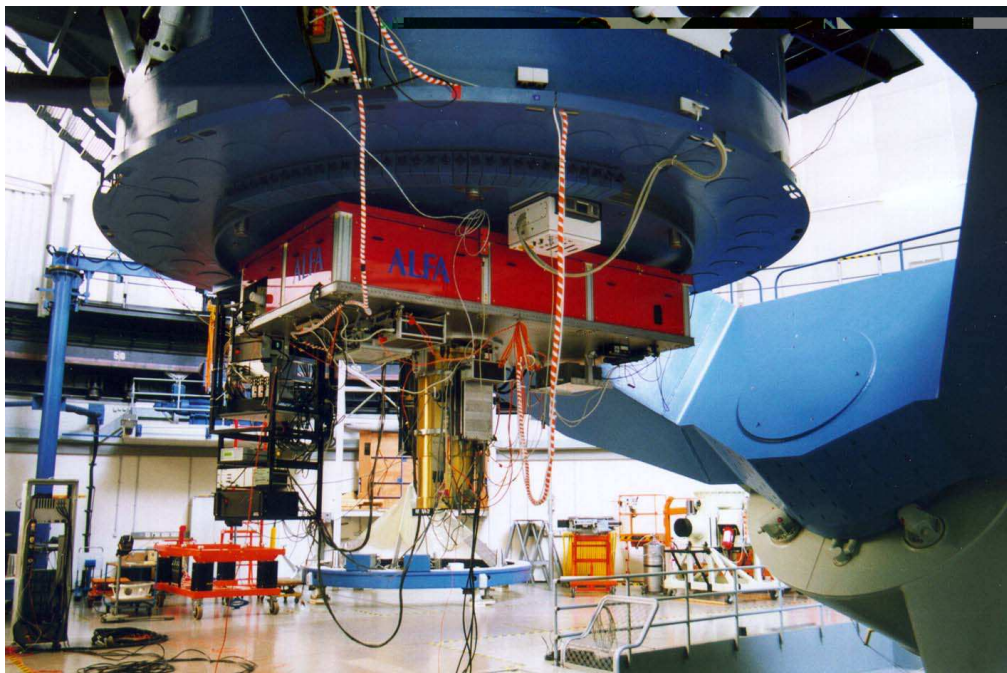


Figure 2. ALFA (rectangular box) and the near-infrared camera OMEGA-Cass (below ALFA) mounted at the Cassegrain flange of the 3.5 m telescope.

### 3. The Measurements

Measurements were done from August 31, 2000 on three consecutive nights. While care was taken that most of the time the same binaries were observed with both instruments, some observations were conducted simultaneously on different objects thus enabling us to see if atmospheric parameters are strongly dependent on the viewing direction.

#### 3.1. Observed Objects

Table 1 lists the relevant properties of the observed binaries. The results presented here represent about 10% of the SCIDAR and 30% of the ALFA measurements taken during our run (the remaining data sets are not yet reduced).

Object	$m_V$	$\Delta m_V$	Separation ["]	Sampling [km]
95 Her	4.3	0.1	6.3	0.28
$\gamma$ Del	4.1	1.0	9.6	0.19
$\gamma$ Ari	4.8	0.0	7.8	0.23
8 Lac	5.3	0.8	22.4	0.08

Table 1. Properties of observed binaries and corresponding height sampling (for a zenith position).

### 3.2. SCIDAR measurements and Data Reduction

SCIDAR observations were nearly continuous during the three observing nights. All frames used here were recorded with an approximate pixel sampling of  $1 \times 1 \text{ cm}^2$  at a frame rate of 305 Hz. The mode of observation was usually to start observing a given binary with normal SCIDAR and to switch lenses afterwards to get a more accurate or complete sampling of the present turbulence structure.

Data reduction was done by a combination of the methods proposed by Klückers et al. (1998) and Avila, Vernin, & Cuevas (1998). First the autocorrelation of the mean-normalized frames of a run is taken and summed up. Then a section parallel and an average section of directions not contributing to the line of separation of the binary's components are extracted and subsequently subtracted to obtain a profile  $A(r)$  that is both background noise reduced and has its central peak eliminated. From this profile, the  $C_n^2(h)$  structure of the atmosphere can be obtained by inversion of the equation:

$$A(r) = \int_{-h_0}^{\infty} C_n^2(h) K(r, h) dh \quad (1)$$

where  $h_0$  is the depth of the virtual conjugate plane and  $K(r, h)$  is a kernel describing the (analytical) profile produced by a layer with a  $C_n^2$  of one at altitude  $h$ . We used a maximum entropy method (MEM) (Avila 2000) for the inversion which generally showed acceptable convergence. In cases where MEM did not converge, a simple least-squares inversion was done. This happened a few times for the second night due to the limited number of data points. Figure 3 shows an autocorrelation (A.C.) profile  $A(r)$  along with the  $C_n^2$  profile obtained from it by inversion of Eq. 1.

Given  $C_n^2(h)$ , the parameters we are interested in can be calculated using (Avila et al. 1998)

$$r_0 = \left[ 0.423 \left( \frac{2\pi}{\lambda} \right)^2 \int dz C_n^2(z) \right]^{-3/5} \quad (2)$$

and (Gonglewski et al. 1990)

$$\theta_0 = 58.1 \times 10^{-3} \lambda^{6/5} \left[ \int dz C_n^2(z) z^{5/3} \right]^{-3/5} \quad (3)$$

where  $\lambda$  is the used wavelength and  $z$  is the height above the telescope.

Although additional information about the turbulence, like wind speeds and a time constant  $\tau_0$  can be extracted from our data, these parameters were not yet calculated for this run as their influence on  $r_0$  and  $\theta_0$  is marginal. However, they do play an important role in selecting an appropriate temporal sampling rate for AO and will thus be addressed in a later publication.

### 3.3. ALFA Measurements and Data Reduction

ALFA was used to measure wavefront gradients and mode contribution both in open-loop and closed-loop. Most of the time the same binaries as with SCIDAR were observed; sometimes, however, we measured a different binary for comparison purposes. Only open-loop data was used to derive  $r_0$  since the procedure is quite straightforward. ALFA was set up to measure with a sampling rate of 300 Hz and a 28-subaperture (one subaperture corresponding to a size of  $\approx 0.5\text{m}$  on the telescope pupil)

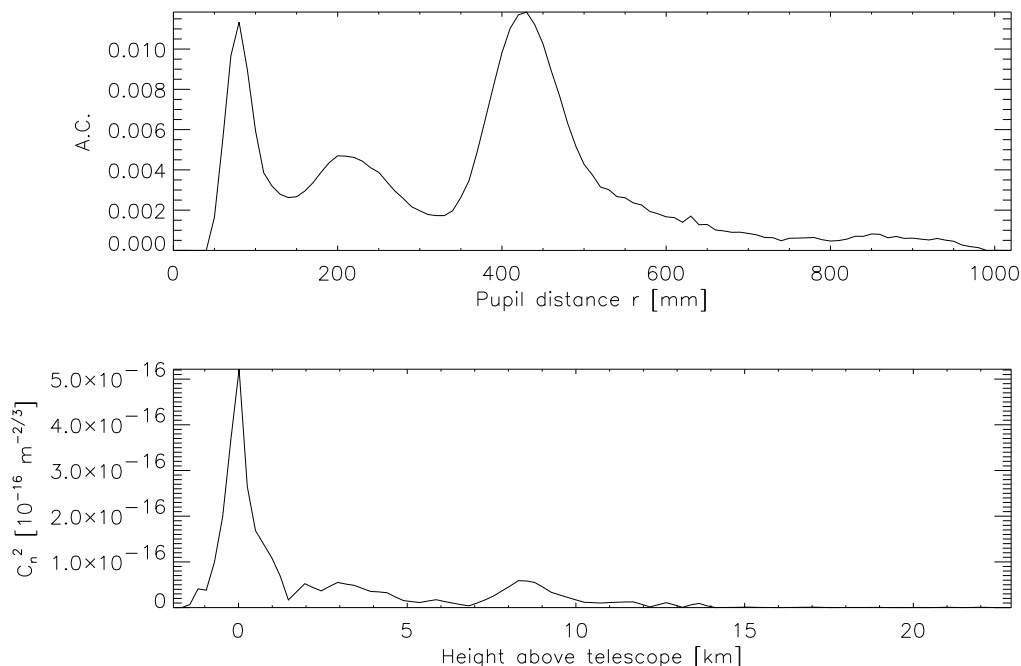


Figure 3. Autocorrelation profile (upper) and  $C_n^2$  profile (lower) obtained from it.

keystone SH lenslet array. The measured modes were of Karhunen-Loève type (Kasper 2000). Typically around 20000 gradients were recorded during one measurement. The Fried parameter  $r_0$  can be determined from these measurements in two distinct ways, one involving the gradients, the other using modal covariances. Determination of  $r_0$  from modal covariances involves the observation that modal covariances scale with  $(D/r_0)^{5/3}$  (Noll 1976), where  $D$  is the telescope diameter; now an iterative scheme was applied that resulted in an estimate for  $r_0$  (Kasper 2000). Alternatively,  $r_0$  was determined from image motion of the subaperture spots as given by the gradients (Glinde-mann et al. 2000).

### 3.4. OMEGA-Cass Measurements and Data Reduction

Along with the ALFA gradient measurements, K-Band images of the binaries were recorded on OMEGA-Cass. The pixel sampling was  $0.08''$  per pixel, appropriate to the maximum obtainable K-Band resolution of  $0.16''$  on a 3.5 m telescope. Due to the binaries brightness, exposure time for a single frame was 1 sec., but integrated frames of varying length have been used here. Only closed-loop images can be used to determine  $\theta_0$ .

In order to find an approximate value for  $\theta_0$ , the *Strehl ratio* of the on-axis  $S_{\text{on}}$  and the off-axis  $S_{\text{off}}$  component of the binary is measured. Using the extended Marechal approximation for the Strehl ratio  $S \approx \exp(-\sigma_p^2)$ , where  $\sigma_p$  denotes the rms wavefront

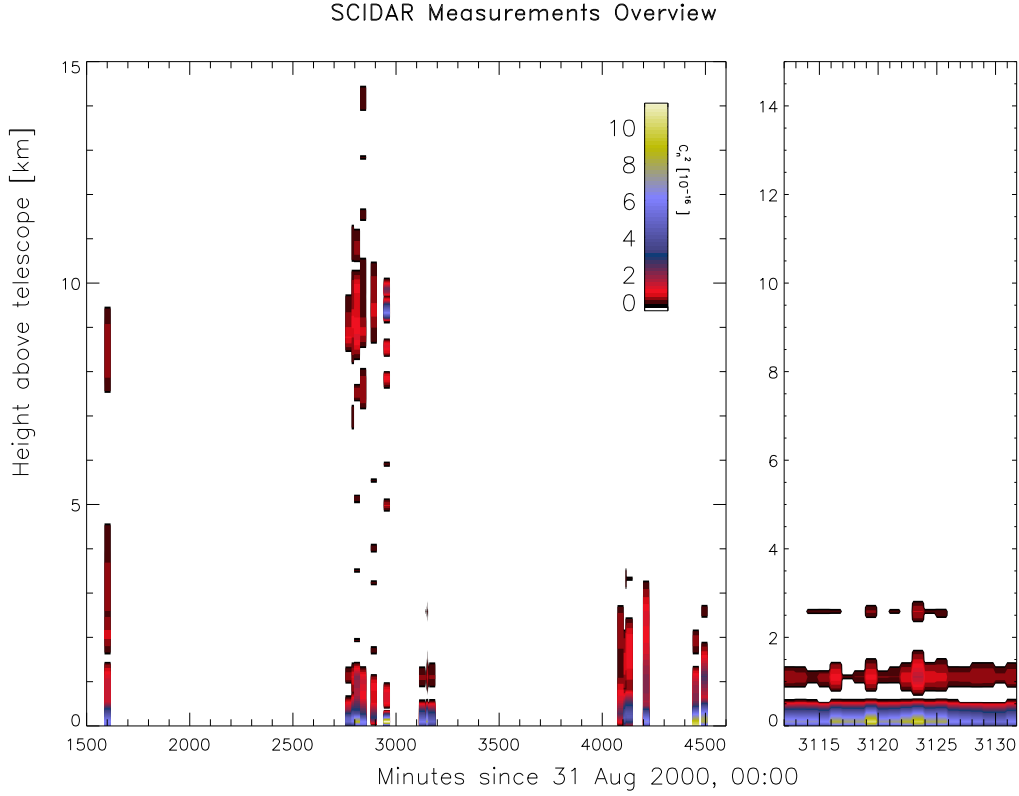


Figure 4. Overview of measured  $C_n^2$  profiles

error, and the expression for the angular isoplanatic error  $\langle \sigma_\theta^2 \rangle = (\theta/\theta_0)^{5/3}$  one gets

$$\theta_0 = \theta \left( \sqrt{\ln \frac{1}{S_{\text{off}}}} - \sqrt{\ln \frac{1}{S_{\text{on}}}} \right)^{-6/5} \quad (4)$$

assuming linear addition of the phase rms errors and  $\theta$  being the separation of the binary components.

## 4. Results

In the following we will shortly describe the results obtained so far. All values have been scaled to zenith viewing direction.

### 4.1. Overview

Figure 4 shows an overview of the measured  $C_n^2$  profiles. The duration of each run has been exaggerated by a factor of 20 for better readability. On the right an enlarged view of the end of the second night is given.

Three main layers can be identified: the ground layer that is present and dominant during all nights and which can be identified with dome seeing, if the cross-correlations

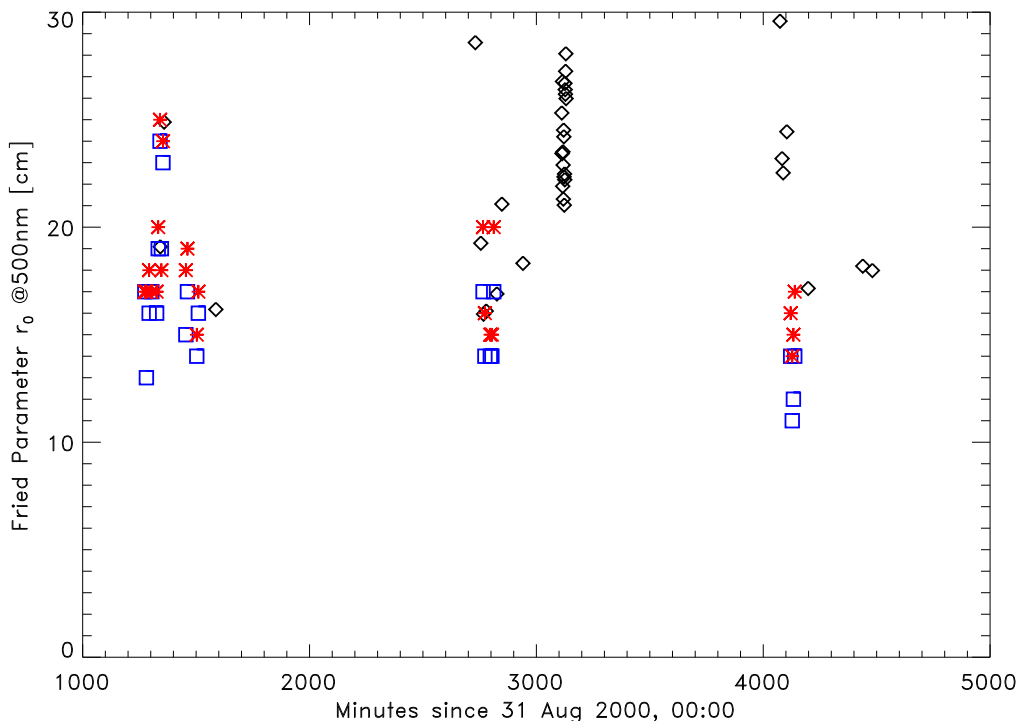


Figure 5. Fried parameter obtained from SCIDAR measurements (diamonds), ALFA modal covariances (squares) and ALFA gradients (asterisks).

show a corresponding static component; a second layer between 1 km and 4 km above the telescope that is fairly extended during the first night, contracts during the second and then extends again in the final night (this layer is well separated from the ground layer as visible in the enlarged view). Finally there is a high layer between 8 and 11 km above the telescope that is gone in the third night. The ground layer is the dominant layer for  $r_0$ ; we therefore expect no significant differences in the behavior of the Fried parameter during the observation period. The disappearing upper layer however should lead to an increase of the isoplanatic angle.

#### 4.2. Fried Parameter $r_0$

Figure 5 shows the measured values of  $r_0$ . A first glance shows that it is strongly varying during a single night which is not much of a surprise. Despite the quite different structure of the turbulence during the three nights as discussed in the previous section, the range of variation seems to be the same. This is clearly due to the dominance of the strong ground layer and possible dome seeing components of  $C_n^2$ , the higher layers being much weaker and therefore only of little importance to  $r_0$ . A second glance reveals that SCIDAR  $r_0$  values generally are a little higher than their ALFA counterparts. Since one would not expect the dome seeing to be worse in a larger dome this may be a hint on a systematic overestimation of  $r_0$  by generalized SCIDAR. However, this conclusion has to wait for the reduction of all data sets.



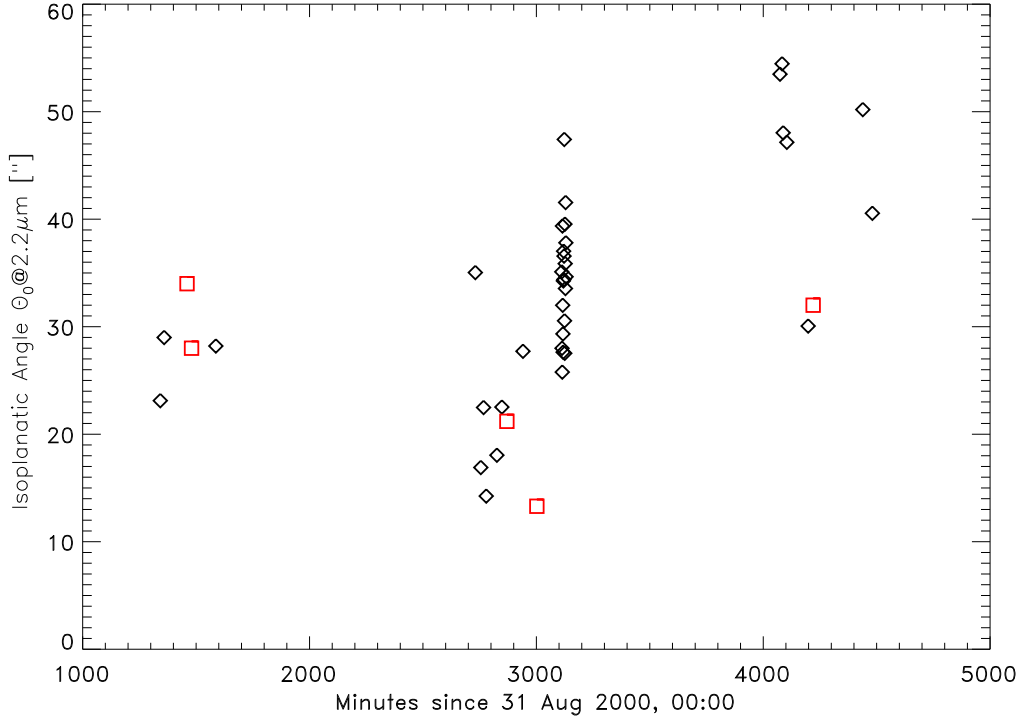


Figure 6. Isoplanatic angle obtained from SCIDAR measurements (diamonds) and from OMEGA-Cass images (squares).

#### 4.3. Isoplanatic Angle $\theta_0$

The measurements of  $\theta_0$  mirror the evolution of the upper turbulent layer, in remaining fairly stable over extended periods of time. As is to be expected from Eq. 3 the presence of the upper turbulent layer results in a relatively low isoplanatic angle of around 22 arcseconds during the first night and the first part of the second night. With its disappearance  $\theta_0$  rises to an average of about 40 arcseconds. At a first glance the agreement between SCIDAR and OMEGA-Cass measurements seems to be even better than for  $r_0$ . However, it has to be said that it turned out to be extremely difficult to infer the isoplanatic angle from Strehl ratio measurements on binaries other than 8 Lac with its large separation of 22.4 arcseconds. The remaining images essentially yielded an infinite  $\theta_0$  which is clearly not sensible.

### 5. Conclusion and Outlook

We have shown that SCIDAR and AO measurements of atmospheric parameters yield similar results. Conclusions as for the use of SCIDAR in assisting AO observations, however, will have to wait until all data sets are reduced. In this process a rigorous error analysis of both ALFA and SCIDAR measurements will be done. Although there are unfortunately only a few data points for isoplanacy measurements with OMEGA-Cass, the tendency and magnitude seem to reproduce SCIDAR results. This gives us hope that approximate PSFs over the whole corrected field of view can really be found

considering SCIDAR data. So the first results of our measurement campaign look quite encouraging.

## **6. Acknowledgements**

The authors thank R. Gredel and H.-W. Rix for their support in re-scheduling this simultaneous observation campaign on Calar Alto.

## **References**

- Avila, R., 2000, private communication.
- Avila, R., Vernin, J., Cuevas, S., 1998, PASP, 110, 1106
- Fuchs, A., Tallon, M., Vernin, J., 1994, Proc. SPIE 2222, 682
- Glindemann, A., Hippler, S., Berkefeld, T., Hackenberg, W., 2000, Experimental Astronomy 10, 5
- Gonglewski, J.D., Voelz, D.G., Fender, J.S., Dayton, D.C., Spielbusch, B.K., Pierson, R.E., 1990, Applied Optics, 29, 4527
- Hippler, S., Glindemann, A., Kasper, M.E., Kalas, P., Rohloff, R.R., Wagner, K., Looze, D.P., Hackenberg, W. 1998, in Proc. of SPIE 3353, Adaptive Optical System Technologies, 44
- Kasper, M.E., 2000, Ph.D. Thesis, Universität Heidelberg
- Kasper, M.E., Looze, D.P., Hippler, S., Herbst, T.M., Glindemann, A., Ott, T., Wirth, A., 2000, Experimental Astronomy 10, 49
- Klückers, V.A., Woeder, N.J., Nicholls, T.W., Adcock, M.J., Munro, I., Dainty, J.C., 1998, A&ASS, 130, 141
- Noll, R.J., 1976, JOSA, 66, 207
- Rocca, A., Roddier, F., Vernin, J., 1974, JOSA, 64, 1000
- Veran, J.-P., Rigaut, F., Maitre, H., Rouan, D., 1997, JOSA A, 73, 3057
- Wirth, A., Navetta, J., Looze, D.P., Hippler, S., Glindemann, A., Hamilton, D., 1998, Applied Optics, 37, 4586